Science of the Total Environment 879 (2023) 163074

Contents lists available at ScienceDirect

Science of the Total Environment

journal homepage: www.elsevier.com/locate/scitotenv

Impact of global urban expansion on the terrestrial vegetation carbon sequestration capacity

Qingwei Zhuang [a], Zhenfeng Shao [a,*], Deren Li [a,b], Xiao Huang [c], Yuzhen Li [d], Orhan Altan [e], Shixin Wu [f]

[a] State Key Laboratory of Information Engineering in Surveying, Mapping and Remote Sensing, Wuhan University, Wuhan 430079, China
[b] School of Remote Sensing and Information Engineering, Wuhan University, Wuhan 430079, China
[c] Department of Geosciences, University of Arkansas, Fayetteville, AR 72701, USA
[d] School of Emergency Management, Xihua University, Chengdu 610039, China
[e] Department of Geomatics Engineering, Istanbul Technical University, Istanbul 36626, Turkey
[f] State Key Laboratory of Desert and Oasis Ecology, Xinjiang Institute of Ecology and Geography, Chinese Academy of Sciences, Urumqi 830011, China

HIGHLIGHTS

- Urban expansion decreases the terrestrial vegetation carbon sequestration capacity.
- The direct decrease in NEP due to the urban expansion offsets the 1.79 % increasing NEP.
- Indirect impact promotes vegetation growth more in original global urban (before 1990).

GRAPHICAL ABSTRACT

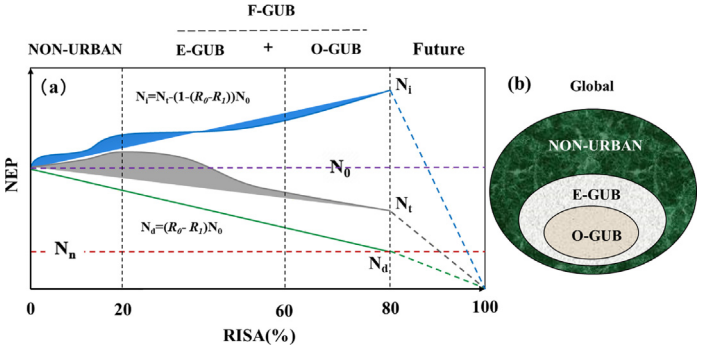

ARTICLE INFO

Editor: Shuqing Zhao

Keywords:
Global change
Urban expansion
Vegetation
Carbon neutrality
Net ecosystem productivity

ABSTRACT

Continuous urban expansion has a negative impact on the potential of terrestrial vegetation. Till now, the mechanism of such impact remains unclear, and there have been no systematic investigations. In this study, we design a theoretical framework by laterally bridging urban boundaries to explain the distress of regional disparities and longitudinally quantify the impacts of urban expansion on net ecosystem productivity (NEP). The findings demonstrate that global urban expanded by 37.60 × 10^4 km^2 during 1990–2017, which is one of the causes of vegetation carbon loss. Meanwhile, certain climatic changes (e.g., rising temperature, rising CO_2, and nitrogen deposition) caused by urban expansion indirectly boosted vegetation carbon sequestration potential through photosynthetic enhancement. The direct decrease in NEP due to the urban expansion (occupying 0.25 % of the Earth's land area) offsets the 1.79 % increase due to the indirect impact. Our findings contribute to a better understanding of the uncertainty associated with urban expansion towards carbon neutrality and provide a scientific reference for sustainable urban development worldwide.

1. Introduction

The terrestrial ecosystem acted as a large net carbon sink in mitigating climate change over the past three decades (Kern and Schlesinger, 1992; Lu et al., 2021; Stocker et al., 2019; Yao et al., 2018). Previous studies have described its carbon sequestration ability in a different manner (Erb et al., 2016; Erb et al., 2018; Tian et al., 2021; Wang et al., 2018). Affected by complex factors (e.g., urbanization (Arneth et al., 2017; Dou et al., 2021), climate change (Ciais et al., 2005; Cox et al., 2013; Doughty et al., 2015; Huang et al., 2019; Xu et al., 2019), and deforestation (Chazdon et al., 2016; Miettinen et al., 2011; Qin et al., 2021)), the impact of

* Corresponding author.
E-mail address: shaozhenfeng@whu.edu.cn (Z. Shao).

http://dx.doi.org/10.1016/j.scitotenv.2023.163074
Received 11 January 2023; Received in revised form 1 March 2023; Accepted 22 March 2023
Available online 24 March 2023

terrestrial vegetation on the global carbon cycle is one of the biggest uncertainties (Brandt et al., 2018; Brovkin et al., 2013; Houghton and Nassikas, 2017). Nevertheless, limited by observational data and simulation models, the spatial-temporal trends and changing mechanisms of global terrestrial vegetation's carbon sequestration potential in the past three decades remain unclear (Chen et al., 2019; Chini et al., 2021; Tagesson et al., 2020). Urban lands have a disproportionate impact on carbon cycling processes in terrestrial ecosystems (Chen et al., 2020; Gong et al., 2020; Liu et al., 2022). Urban expansion can cause vegetation cover loss and other irreversible biophysical and biochemical processes (Cai et al., 2022; Endreny, 2018; Li et al., 2017a). However, urban expansion is featured by high spatial heterogeneity (Gregg et al., 2003; Xu et al., 2017), and it is a serious challenge to investigate the impact of global urban expansion on the carbon sequestration capacity of vegetation.

Some existing studies have proved that urban expansion has a negative impact on the vegetation carbon sequestration capacity (Lai et al., 2016; Luo et al., 2021; Yan et al., 2021; Zhuang et al., 2022). Imhoff et al. (2004) proved that urban expansion is taking place on the most fertile lands and hence has a disproportionately large overall negative impact on Net Primary Productivity (NPP) in the United States. Seto et al. (2012) thought that urban land-cover change threatens biodiversity and affects ecosystem productivity through loss of habitat, biomass, and carbon storage. Wen et al. (2019) found that urban expansion significantly offset the climate change-induced NPP increases and worsened NPP decreases (the offsetting ratio calculated for China was 5.42 %). However, these studies focus on the direct impacts caused by the urban land conversion. Zhao et al. (2016) defined the direct impact as the LULC effect of urbanization, and the indirect impact was regarded as the influence of other factors, such as climate change, anthropogenic activities, and so on. This perspective provides new ideas for exploring the impact of global and regional urban expansion on carbon budgets. We also argue that designing a more rational framework to distinguish different impacts would be more conducive to a systematic understanding of the impact of urbanization on regional carbon budgets.

This study fills this gap by developing a theoretical framework that spans urban boundaries to investigate the impact of urban expansion on the terrestrial vegetation's carbon sequestration potential. The proposed theoretical framework is expected to strengthen the understanding of the response of global-scale net ecosystem productivity (NEP) to urban expansion by setting natural control experiments (e.g., warming, CO_2 emissions, and nitrogen deposition) (Surawski et al., 2016; Wang et al., 2019; Wohlfahrt et al., 2019). The Global Impervious Surface Area (GISA) dataset is a newly developed dataset using >3,000,000 Landsat series images, featured by fine spatial-temporal granularity and a long time span (Huang et al., 2021). This dataset allows us to analyze the global urban expansion from 1990 to 2017 with great accuracy. Then, multi-period urban boundaries were delineated via joint kernel density estimation (KDE), cellular automata (CA), and morphology (Li et al., 2020). The global NEP dataset was simulated using vegetation parameters, meteorological data, and atmospheric CO2 concentration to drive the mechanistic ecological model (Chen et al., 2019; He et al., 2021). We analyze the impact of urban expansion on NEP by laterally crossing urban boundaries to explain the distress of regional differences. In addition, the impacts of urban expansion on fixed-region NEP were longitudinally quantified to compensate for the lack of global-scale control experiments. The answers given by this study are crucial for assessing the Sustainable Development Goals (SDGs), benefiting the achievement of "carbon neutrality" of global ecosystems.

2. Material and methods

2.1. Global impervious surface datasets

The global impervious surface dataset was obtained from the Institute of Remote Sensing Information Processing, Wuhan University. It was produced using >3,000,000 Landsat images with 0.00026949459° × 0.00026949459° spatial resolution on the Google Earth Engine (GEE) platform (Huang et al., 2021). Based on 120,777 points randomly selected from 270 cities around the world, the false alarm rate, false alarm rate, and F-score are 5.16 %, 0.82 %, and 0.95 %, respectively. Such an accuracy can meet the needs of this study.

2.2. Global NEP datasets

The global NEP dataset was obtained from the International Institute for Earth System Sciences, Nanjing University. It was produced using vegetation parameters, meteorological data, and atmospheric CO2 concentration to drive the daily step-length boreal ecosystem productivity simulator (BEPS) model (Chen et al., 2019; He et al., 2021). It has a temporal resolution of daily, and a spatial resolution of 0.072727° × 0.072727°. R^2 and nRMSE (RMSE/STD) between the simulated NEP and 462 site years were 0.76 ($n = 462$, $p < 0.001$) and 0.53, respectively. The spatial resolution of this dataset has been resampled to 0.00026949459° × 0.00026949459° via cubic convolution interpolation before all calculations are performed. The accuracy verification results after resampling are shown in Fig. S2.

2.3. Global urban boundaries

The global urban boundaries were collected from Tsinghua University (Li et al., 2020). The methods used to delineate urban boundaries can be roughly divided into three categories: (1) based on population density; (2) based on the night-time light (NTL) satellite data; and (3) based on land cover data. The urban boundary data selected for this study was constructed through the global artificial impervious area with a spatial resolution of 0.00026949459° × 0.00026949459° (Gong et al., 2020). The derived urban boundary around urban fringe areas was improved by using a morphological approach (Liang et al., 2018; Musikhin and Karpik, 2023). The urban boundaries from this dataset are highly consistent with the results from NTL data and human interpretation. So this dataset was used in this study.

2.4. Spatial-temporal dynamics of NEP during the study period

We used the one-dimensional linear regression method to perform a time series analysis of NEP since 1990. The trend rate was used to characterize the spatial-temporal trend of NEP. A positive or negative trend rate indicates an increasing or decreasing NEP during the study period. Meanwhile, the magnitude of the trend rate reflects the rate of increase or decrease of NEP. The trend slope is calculated as (Feng et al., 2022):

$$\theta_{\text{slope}} = \frac{n \times \sum_{i=1}^{n} x_i t_i - \sum_{i=1}^{n} x_i \sum_{i=1}^{n} t_i}{n \times \sum_{i=1}^{n} t_i^2 - \left(\sum_{i=1}^{n} t_i\right)^2} \tag{1}$$

where θ_{slope} is the trend slope; n refers to the length of time series; x_i denotes the NPP in year i; t_i is the ith year.

Fluctuation analysis follows:

$$CV = \frac{1}{\overline{NEP}} \times \sqrt{\frac{\sum_{i=1}^{n} \left(NEP_i - \overline{NEP}\right)^2}{n-1}} \tag{2}$$

where CV is the coefficient of variation; n is the length of the time series; i represents the ith year; NEP_i denotes the NEP in year i; $\overline{NEP}$ is the average NEP during the study period.

F-test follows:

$$F = \sum_{i=1}^{n} \left(\overleftrightarrow{x_i} - \overline{x}\right)^2 \times \frac{n-2}{\sum_{i=1}^{n} \left(x_i - \overleftrightarrow{x_i}\right)} \tag{3}$$

where n represents the total number of years; x_i is the annual NEP in the ith year; $\overleftrightarrow{x_i}$ is the annual regression NEP in the ith year; $\overline{x}$ refers to mean NEP during the investigated period.

2.5. Loss of vegetation carbon sequestration capacity by urban expansion

We quantified the NEP loss due to urban expansion by using the land use transfer matrix and the net ecosystem productivity loss formula. This correlation model is very reliable in exploring the relationship between two variables. The evaluation process was as follows:

$$\Delta NEP = \Sigma A_{ISA} \times \left(NEP_{(i,t_2)} - NEP_{(i,t_1)}\right) \tag{4}$$

where ΔNEP is the NEP loss due to urban expansion; A_{ISA} refers to the area of ISA; $NEP_{(i,t_1)}$ denotes the NEP of the ith pixel at time t_1 ($gC{\cdot}m^{-2}{\cdot}year^{-1}$); $NEP_{(i,t_2)}$ denotes the NEP of the ith pixel at time t_2 ($gC{\cdot}m^{-2}{\cdot}year^{-1}$).

$$DY_t = \frac{ISA_{t_2} - ISA_{t_1}}{ISA_{t_1}} \times \frac{1}{t_2 - t_1} \times 100\ \% \tag{5}$$

where DY_t indicates the dynamic attitude of ISA (%); ISA_{t_1} and ISA_{t_2} represents the area of ISA in t_1 and t_2 (km^2).

The impact of urban sprawl on NEP (IM_t) is given by the following equations:

$$IM_t = \frac{\Sigma\left(NEP_{(i,t1)} + NEP_{(i,t_2)}\right)}{2\Delta NEP} \tag{6}$$

$$I = \frac{\sum_{i=1}^{n}\sum_{i\neq 1}^{n}\omega_{ij}(\chi_i - \overline{\chi})\left(\chi_j - \overline{\chi}\right)}{S^2\sum_{i=1}^{n}\sum_{i\neq 1}^{n}\omega_{ij}} \tag{7}$$

$$I_i = \frac{(\chi_i - \overline{\chi})\sum_{i\neq 1}^{n}\left(\chi_j - \overline{\chi}\right)}{S^2} \tag{8}$$

$$S_i^2 = \frac{1}{n}\Sigma_i(\chi_i - \overline{\chi})^2 \tag{9}$$

$$G_i = \frac{\sum_{i\neq 1}^{n}\omega_{ij}\chi_j}{\sum_{i\neq 1}^{n}\chi_j} \tag{10}$$

where I and I_i are the global Moran's I and local Moran's I; G_i is the statistic of local G_i index; χ_i is the NEP loss in grid i during the study period; $\overline{\chi}$ is the average of all pixel NEP losses; ω_{ij} denotes the spatial weights between grid i and grid j; n is the number of grids; S_i^2 is the variance of NEP loss within grid i.

3. Results

3.1. Global urban expansion during 1990–2017

Impervious surface area (ISA) is a direct physical indicator of urban expansion. We found that the global ISA expanded by 37.60 × 10^4 km^2 (42.40 × 10^4 km^2 in 1990 and 80.00 × 10^4 km^2 in 2017), and the increasing ratio reached 88.69 %. Urban expansion exhibits high spatial heterogeneity across continents, with the fastest growth in Asia (Fig. 1). North America was the second-largest contributor to global urban expansion, with 9.11 × 10^4 km^2 of land converted to urban lands. Asia (49.82 %) and North America (24.22 %) combined accounted for 74.04 % of the global expanded ISA from 1990 to 2017. It should be noted that Africa is the continent with the fastest relative urban expansion in the world. The ISA in Africa increased by 2.24 × 10^4 km^2, and the expansion rate reached 167.86 % of that in 1990. In addition, the urban expansion in South America (89.66 %) is close to the global average (88.69 %). Urban expansion in Europe with the slowest rate, which is considerably lower than the global average expansion rate.

The multi-temporal urban boundaries were mapped using the ISA dataset. We further explored the differences in ISA among the original global urban boundary (termed O-GUB) in 1990, the expanded global urban boundary (termed E-GUB) from 1990 to 2017, and the final global urban boundary (termed F-GUB) in 2017. Fig. 2 shows that the variability of ISA across urban boundaries is notably higher than that of continental scales. Specifically, the ISA in the F-GUB expanded by 17.23 × 10^4 km^2 (from 27.94 × 10^4 km^2 to 45.17 × 10^4 km^2), and the percentage of ISA (PISA, which represents the proportion of ISA to this region) increased from 35.02 % to 56.62 % during the investigated period. In O-GUB, the ISA expanded slowly during the investigated period (3.57 × 10^4 km^2) — the slowest of the three GUBs. The ISA expansion in E-GUB is 13.65 × 10^4 km^2, accounting for about 80 % of the total expanded ISA in global urban areas during the investigated period. Thus, E-GUB should be considered as the typical area for studying ISA changes. Variations in ISA expansion across urban boundaries are expected to introduce different impacts on the vegetation carbon storage capacity.

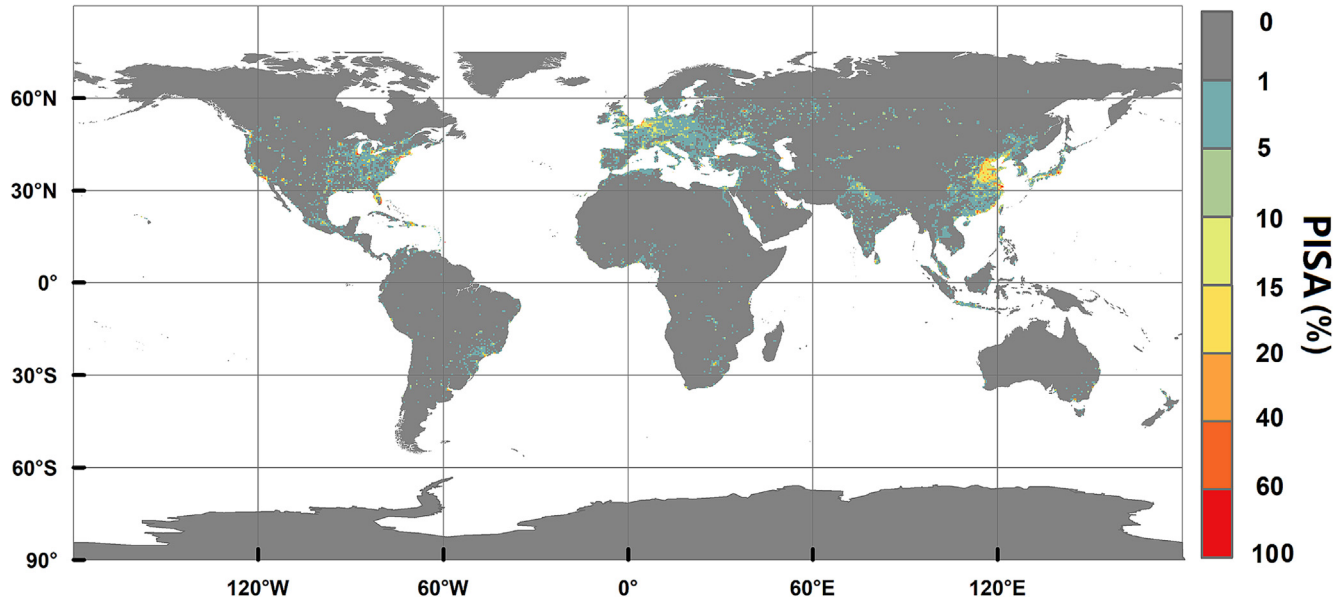

Fig. 1. The percentage of ISA (PISA) (with 0.5° × 0.5° as spatial resolution) by comparing 2017 with 1990.

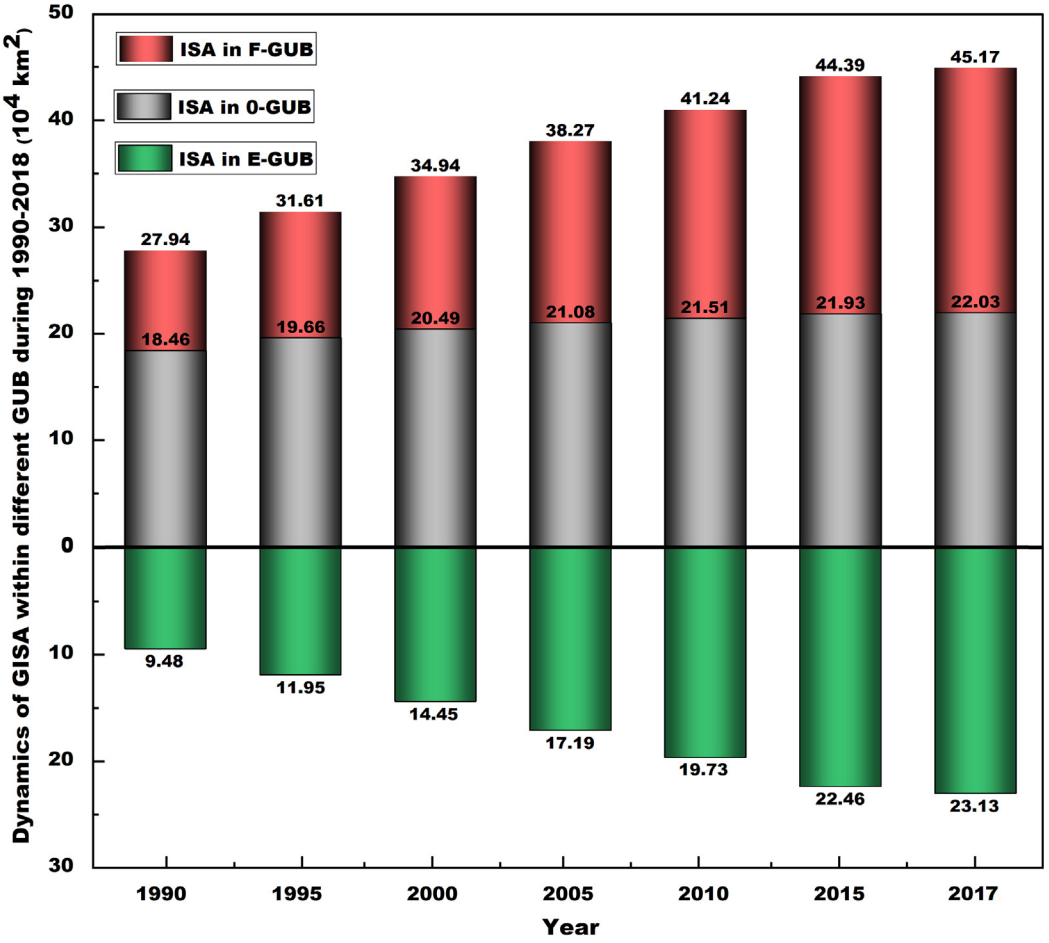

Fig. 2. Temporal heterogeneity of ISA in the global urban boundaries. Note: O-GUB denotes original global urban boundaries in 1990; F-GUB denotes final global urban boundaries in 2017; E-GUB denotes expanded global urban boundaries from 1990 to 2017.

3.2. Spatial-temporal variations of global NEP

The NEP was studied from 1990 to 2017 to assess the terrestrial vegetation carbon sequestration potential. The results indicate that terrestrial vegetation presented a notable carbon sink capacity during the investigated period, with an average annual net absorption of 13.81 Pg C from the atmosphere. From the spatial distribution, Asia is becoming the dominant contributor to the global terrestrial carbon sink. Afforestation policies in China made a particularly positive contribution, while deforestation policies in Southeast Asia played a negative role (Fig. 3a). It is worth mentioning that vegetation in North America and Europe also revealed a stable carbon sink during the investigated period. In terms of the proportion of positive and negative pixel changes, 61.36 % of the pixels had a positive trend in NEP, with 44.09 % having a growth rate >4 gC·m^{-2}·year^{-1} (Fig. 3b). 38.64 % of the total pixels had a negative trend in NEP, with 1.49 % having a decrease >4 gC·m^{-2}·year^{-1}. More specifically, the trends of inter-annual fluctuations in NEP by continent are shown in Fig. S1.

3.3. Impact of urban expansion on vegetation carbon sequestration potential

Despite the fact that urban areas make up only a minor percentage of the worldwide land surface (0.54 %), their expansion can weaken the growth rate of terrestrial NEP due to the reduction of vegetation caused by the land cover conversion. The carbon sequestration potential of terrestrial vegetation may be affected by environmental change and human activities due to urban expansion. For the retained vegetation area, the carbon sequestration potential also revealed varied patterns. The purple line represents the yearly mean offset from the initial NEP in F-GUB and the brown line represents the yearly mean offset from the initial NEP in non-urban areas notably present different patterns, suggesting the disparity in the change rate of NEP between urban and non-urban areas (Fig. 4a). The growth rate of NEP in non-urban areas (θ = 0.543) is considerably higher than that in urban areas (θ = 0.161). Inside the urban areas, the average NEP at the pixel scale increased by 12.15 gC·m^{-2}·year^{-1} in O-GUB. In comparison, the average NEP at the pixel scale only increased by 2.71 gC·m^{-2}·year^{-1} in E-GUB (Fig. 4b). The different growth rates and increments of NEP at the pixel scale demonstrate that urban expansion does have different impacts on the vegetation's carbon sequestration potential.

The conceptual results indicated that the direct impact of urban expansion on NEP is negative, whereas the indirect impact is likely to strengthen the increase of NEP. For terrestrial ecosystems, the direct decrease in NEP caused by urban expansion offsets 1.79 % of the indirect increase. Such offsets show clear discrepancies across urban boundaries. In O-GUB, the offset ratio reached 25.21 %. In E-GUB, this rate is as high as 234.35 %, indicating that the vegetation carbon storage is on a downward trend during the investigated period. Non-urban areas present a weak offsetting effect (0.91 %) of direct impacts on indirect impacts. This indirect effect on the promotion of vegetation photosynthesis is expected to reach a saturation state after PISA reaches a certain threshold. After reaching the saturation state, the vegetation's carbon sequestration potential is likely to shapely drop following the continuous increase of PISA.

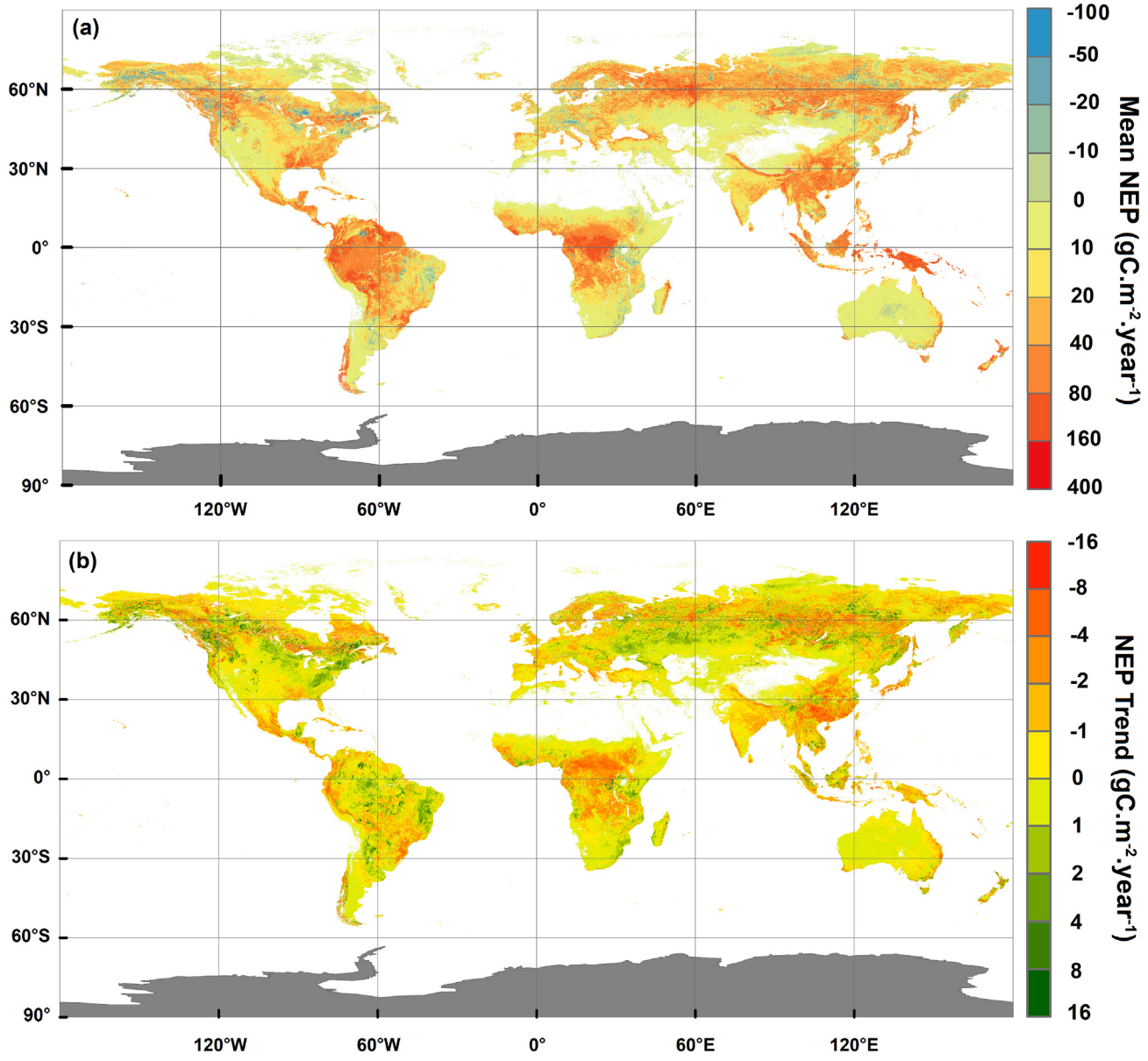

Fig. 3. (a) Spatial distribution of mean NEP; (b) inter-annual variations of NPP during 1990–2017.

4. Discussion

4.1. Necessity of isolating the direct and indirect impact of urban expansion on the terrestrial vegetation carbon sequestration capacity

Urban expansion irreversibly alters the biogeochemical cycles and photosynthetic productivity of terrestrial ecosystems (Chen et al., 2013; Di Vittorio et al., 2018; Di Vittorio et al., 2020; Li et al., 2021). The direct and indirect impacts of urban expansion on NEP have been proven to exist (Buyantuyev and Wu, 2009). It is easy to understand that the direct impact refers to the loss of carbon caused by the transformation of the vegetation surface into urban lands. The intensity of the direct impact is proportional to the vegetation loss area and the vegetation NEP before the loss. The process of indirect impact is more complicated compared with direct impact, as the indirect impact is not clearly defined leading to its difficulty in measurement. The overall impact into direct and indirect impacts is of great importance in investigating vegetation carbon sequestration potential. Efforts have been made to distinguish these two impacts using operational experiments and comparative urban-rural analysis (Guan et al., 2019; Wen et al., 2019; Zhao et al., 2016). Building upon existing works, we designed a theoretical framework to isolate direct and indirect impacts through crossing urban boundaries (Fig. 5a).

4.2. How much does global urban expansion affect the carbon sequestration capacity of terrestrial vegetation?

A past study has shown that newly urbanized areas covered 0.04 % of the Earth's terrestrial surface, and the urbanization-induced decrease in NPP offset 30 % of the climate-driven increase from 2000 to 2010 (Liu et al., 2019). Zhang et al. (2022) pointed out that while the amount of urban vegetation has been decreasing from 2001 to 2018 as a direct result of human urbanization and development, vegetation growth (vegetation “greenness” as observed by remote sensing) within cities has been increasing. This implies a broad positive indirect effect of the urban environment on vegetation growth (average enhancement of about 26 % at the global scale). However, this effort potentially overestimated the impact of urban expansion on vegetation

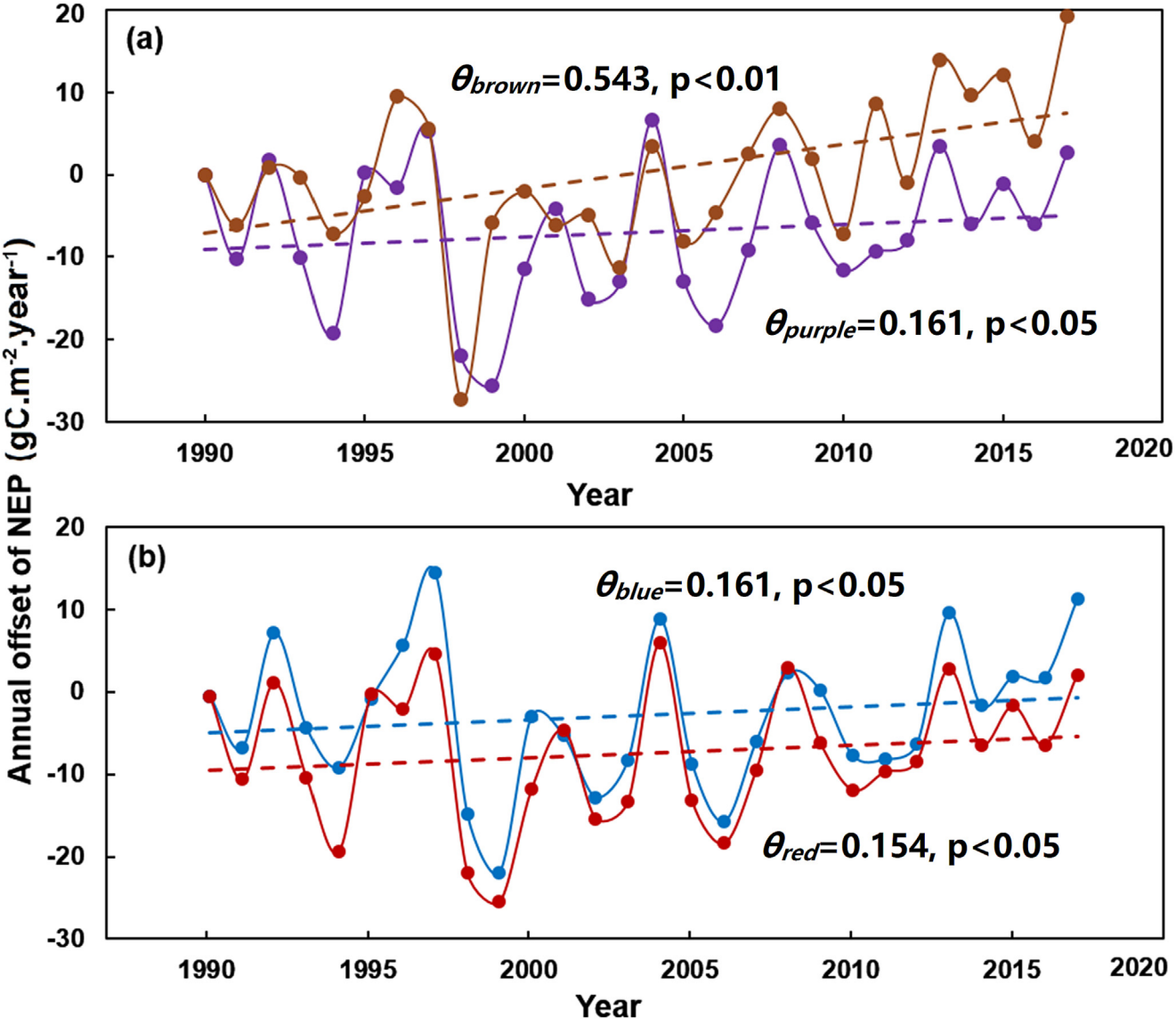

Fig. 4. Annual offsets of mean NEP from 1990 to 2017 through crossing global urban boundaries. (a) NEP offsets in non-urban areas and F-GUB; (b) NEP offsets in O-GUB and E-GUB. The brown line represents the annual mean offset from the initial NEP in non-urban areas. The purple line indicates the annual mean offset from the initial NEP in F-GUB. The green line and the red line represent the year-by-year offset from the initial NEP in O-GUB and E-GUB, respectively. θ indicates the annual change rate of NEP.

productivity. Our study also reveals urban expansion can offset some of the indirect impacts of vegetation carbon sequestration, and we believe that a theoretical framework across urban boundaries can lead to more reasonable results. The results can be supported by numerous efforts from terrestrial ecosystems (Le Noe et al., 2021), urban ecosystems (Donato et al., 2011; Li et al., 2017b; Tong et al., 2020), and national scales (Tang et al., 2021). Overall, the direct reduction in NEP due to the expanded urban lands (0.25 % of the earth's land area) offsets the 1.79 % increase due to indirect effects, which is consistent with the predictions based on CMIP5 data (Quesada et al., 2018). The offsetting results vary greatly across different urban boundaries (Fig. 5b). Along the Earth's radius, the direct decrease can offset 25.21 % of the indirect increase in O-GUB. Such an offsetting effect can reach 40 % and 29.9 % in China and the United States (Jia et al., 2018; Zhao et al., 2016), where the ISA expanded the fastest. For E-GUB, where intensive urban expansion happens the carbon loss directly caused by the destruction of vegetation (3.07 Pg C) is much higher than the carbon increase caused by the indirect impact (1.31 Pg C). In non-urban areas, the direct impact offset 0.91 % of the indirect increase. Such a low offsetting effect can be explained by the extremely small ratio of ISA and vegetation area ([0.32 % in 1990, 0.76 % in 2017]) in non-urban areas.

4.3. Strengths and new perspectives of this study

Although extensive studies have been conducted to demonstrate that urban expansion (urbanization or major transfer types in land-use change) has an impact on vegetation carbon sequestration potential, the impact mechanism of urban expansion on the vegetation carbon sequestration potential remains unclear at the global scale. Compared with existing efforts in Table 1, our study has the following advantages: (1) superiority in data: the selected NEP is closer to the actual vegetation carbon sink than gross primary productivity (GPP) and net primary productivity (NPP). The relationship between NEP, GPP, and NPP can be found in this reference (Yu et al., 2011). (2) Innovative methodological design: we established a new theoretical framework for crossing urban boundary investigations. The superiority of this method lies in the zoning discussion of terrestrial ecosystems by coupling multi-temporal urban boundaries. In addition, the divisional discussion of

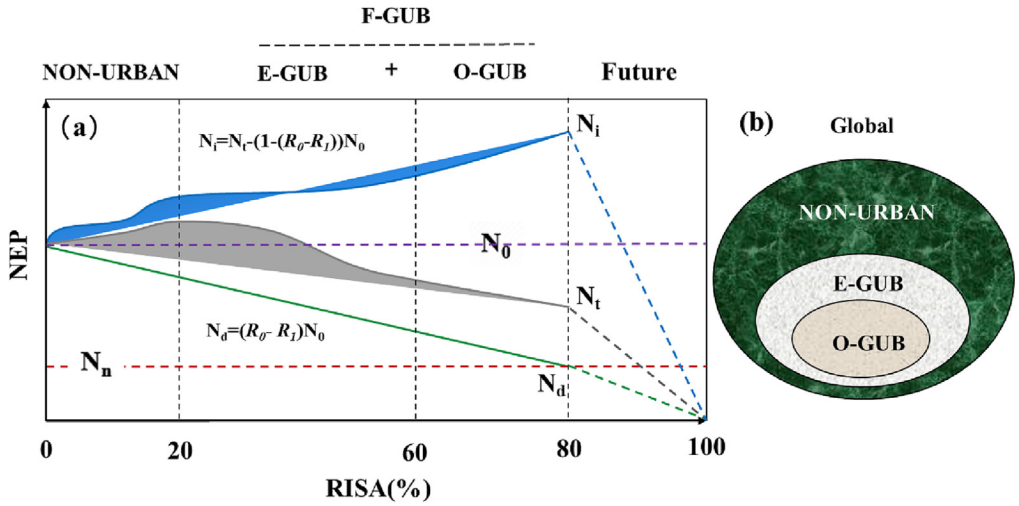

Fig. 5. Conceptual diagram that reveals the impacts of urban expansion on vegetation carbon sequestration potential through crossing urban boundaries analysis. (a) N_0 and N_n represent mean NEP in non-urban areas and highly urbanized areas, respectively. (b) A conceptual diagram of crossing urban boundaries. N_d, N_i, and N_t represent the NEP that is only directly affected, the NEP that is only indirectly affected, and the actual NEP at time t, respectively. The green line and the blue line represent the NEP controlled by the direct and indirect impacts of urban expansion, respectively. The grey line denotes the actual NEP across urban boundaries as PISA increases. The black dashed line represents the approximate PISA across the boundaries. O-GUB: the original global urban boundary in 1990; E-GUB: the expanded global urban boundary from 1990 to 2017; F-GUB: the final global urban boundary in 2017.

the terrestrial ecosystem through the coupling of multi-temporal urban boundaries leads to more reasonable explanations.

4.4. Limitations and future direction

We reveal the impact of urban expansion on the carbon sequestration potential of terrestrial vegetation by establishing a new methodology in this research. Nevertheless, the distinction between direct and indirect impacts is often hampered by unknown factors. E.g., indirect impacts are complex and many environmental factors can significantly influence the spatial and temporal dynamics of NEP. In addition, the transition from non-urban to urban land is highly complex and spatially heterogeneous, and the limited number of urban ecosystem eddy towers may not be sufficient to fully capture its spatial and temporal variables. In addition to urban sprawl, additional factors should be considered in future studies, including vegetation structure, climate change, soil conditions, and nitrogen deposition. We also call for the protection and enhancement of urban vegetation. If they continue to be destroyed, they may cause an irreversible decrease in vegetation carbon sink capacity.

5. Conclusion

This study demonstrated that urban sprawl has complex effects on the carbon sequestration potential of vegetation. It has both theoretical and practical implications for sustainable urban development and global carbon neutrality. We found that global cities have expanded by 88.69 % in the last three decades. More than half of the expanding ISAs have occurred in Asia and North America. A conceptual framework based on cross-urban boundaries suggests that urban sprawl reduces the growth rate of vegetation's carbon sequestration capacity. In detail, the direct decrease in NEP caused by global urban expansion offsets 1.79 % of the indirect increase. Such offsets show clear discrepancies across urban boundaries, the offset ratio reached 25.21 %, 234.35 %, and 0.91 % in O-GUB, E-GUB, and non-urban areas, respectively. These results are more accurate and detailed when compared to the results of existing studies. They can provide viable recommendations for sustainable and carbon-neutral communities worldwide.

Funding

This work was supported in part by the National Natural Science Foundation of China under Grants 42090012 and 42205127; China Association for Science and Technology (20220615ZZ07110306); Key R&D Project of Sichuan Science and Technology Plan (2022YFN0031); and Natural Science Foundation of Sichuan (2022NSFCSC1124).

CRediT authorship contribution statement

All authors contributed to the study conception and design. Q. Zhuang, Z. Shao and D. Li designed the research; X. Huang, Y. Li and S. Wu performed experiments and computational analysis; Q. Zhuang drafted the paper; Q. Zhuang and O. Altan contributed to the interpretation and the preparation of the manuscript.

Table 1
Existing efforts in investigating the impacts of ISA expansion (urbanization or land-use change) on vegetation conditions.

Variable	Spatial scales	Period	Impacts	References
Calories	Global	2000	Urbanization reduced crop yields by 3–4 %.	(d'Amour et al., 2017)
NPP	Global	2000–2010	The urbanization-induced decrease in NPP offsets 30 % of the climate-driven increase	(Liu et al., 2019)
NPP	Global	2006–2100	Global net primary productivity is found to be only slightly affected by LULCC	(Quesada et al., 2018)
Biomass	Pan-tropics	2000–2030	Urbanization resulted in a loss of 1.38 Pg C of biomass carbon	(Seto et al., 2012)
NPP	USA	1992–1993	Urban land transformation in the US has reduced NPP by 1.6 % of the pre-urban input.	(Imhoff et al., 2004)
EVI	377 cities in the USA	2001, 2006, & 2011	Indirect impacts offset about 29.9 % of the direct negative impacts of urbanization on vegetation	(Jia et al., 2018)
NPP	China	1989–2000	NPP lost 0.95 Tg directly, not taking into account indirect effects	(Tian and Qiao, 2014)
NPP	China	2000–2010	Urban expansion significantly offset 5.42 % of the climate change-induced NPP increases	(Wen et al., 2019)
EVI	32 Chinese cities	2001, 2006, & 2011	Indirect impact offsets about 40 % of the direct negative impacts of urbanization on vegetation	(Zhao et al., 2016)

Note: EVI, enhanced vegetation index; NPP, net primary productivity.

Data availability

The multi-period global urban boundaries are available from http://data.ess.tsinghua.edu.cn/. The historical global impervious surface area (ISA) datasets are available from http://irsip.whu.edu.cn/resources/dataweb.php. The historical net ecosystem productivity (NEP) datasets were available from http://www.nesdc.org.cn/sdo/detail?id=612f42ee7e28172cbed3d80d. Annual GPP derived from measurements at flux towers using the eddy covariance technique are available from the FLUXNET 2015 database (http://fluxnet.fluxdata.org/data/fluxnet2015-dataset/) and ChinaFlux database (http://www.chinaflux.org/general/index.aspx?nodeid=12). Remotely sensed LAI are available from http://www.resdc.cn/data.aspx?DATAID=336. Daily maximum temperature, minimum temperature, solar radiation, precipitation, and daily average relative humidity are available from https://catalogue.ceda.ac.uk/uuid/10d2c73e5a7d46f4ada08b0a26302ef7. Soil datasets are available from http://www.fao.org/nr/lman/abst/lman_080701_en.htm.

Declaration of competing interest

The authors declare no conflict of interest. The funding sponsors had no role in the design of the study, in the collection, analyses, or interpretation of the data, in the writing of the manuscript, or in the decision to publish the results.

Acknowledgments

We would like to extend sincere gratitude to the academic editor and reviewers for their constructive comments which greatly helped us to improve the quality of this manuscript. Thanks to Professor Peng Gong of Tsinghua University, Professor Weimin Ju of Nanjing University, and Professor Xin Huang of Wuhan University for providing the datasets used in the research.

Appendix A. Supplementary data

Supplementary data to this article can be found online at https://doi.org/10.1016/j.scitotenv.2023.163074.

References

Arneth, A., Sitch, S., Pongratz, J., Stocker, B.D., Ciais, P., Poulter, B., Bayer, A.D., Bondeau, A., Calle, L., Chini, L.P., Gasser, T., Fader, M., Friedlingstein, P., Kato, E., Li, W., Lindeskog, M., Nabel, J.E.M.S., Pugh, T.A.M., Robertson, E., Viovy, N., Yue, C., Zaehle, S., 2017. Historical carbon dioxide emissions caused by land-use changes are possibly larger than assumed. Nat. Geosci. 10, 79.

Brandt, M., Rasmussen, K., Hiernaux, P., Herrmann, S., Tucker, C.J., Tong, X., Tian, F., Mertz, O., Kergoat, L., Mbow, C., David, J.L., Melocik, K.A., Dendoncker, M., Vincke, C., Fensholt, R., 2018. Reduction of tree cover in West African woodlands and promotion in semi-arid farmlands. Nat. Geosci. 11, 328.

Brovkin, V., Boysen, L., Arora, V.K., Boisier, J.P., Cadule, P., Chini, L., Claussen, M., Friedlingstein, P., Gayler, V., van den Hurk, B.J.J.M., Hurtt, G.C., Jones, C.D., Kato, E., de Noblet-Ducoudre, N., Pacifico, F., Pongratz, J., Weiss, M., 2013. Effect of anthropogenic land-use and land-cover changes on climate and land carbon storage in CMIP5 projections for the twenty-first century. J. Clim. 26, 6859–6881.

Buyantuyev, A., Wu, J., 2009. Urbanization alters spatiotemporal patterns of ecosystem primary production: a case study of the Phoenix metropolitan region, USA. J. Arid Environ. 73, 512–520.

Cai, B., Shao, Z., Fang, S., Huang, X., Tang, Y., Zheng, M., Zhang, H., 2022. The Evolution of urban agglomerations in China and how it deviates from Zipf's law. Geo-Spat. Inf. Sci https://doi.org/10.1080/10095020.2022.2083527.

Chazdon, R.L., Broadbent, E.N., Rozendaal, D.M.A., Bongers, F., Almeyda Zambrano, A.M., Aide, T.M., Balvanera, P., Becknell, J.M., Boukili, V., Brancalion, P.H.S., Craven, D., Almeida-Cortez, J.S., Cabral, G.A.L., de Jong, B., Denslow, J.S., Dent, D.H., DeWalt, S.J., Dupuy, J.M., Duran, S.M., Espirito-Santo, M.M., Fandino, M.C., Cesar, R.G., Hall, J.S., Hernandez-Stefanoni, J.L., Jakovac, C.C., Junqueira, A.B., Kennard, D., Letcher, S.G., Lohbeck, M., Martinez-Ramos, M., Massoca, P., Meave, J.A., Mesquita, R., Mora, F., Munoz, R., Muscarella, R., Nunes, Y.R.F., Ochoa-Gaona, S., Orihuela-Belmonte, E., Pena-Claros, M., Perez-Garcia, E.A., Piotto, D., Powers, J.S., Rodriguez-Velazquez, J., Romero-Perez, I.E., Ruiz, J., Saldarriaga, J.G., Sanchez-Azofeifa, A., Schwartz, N.B., Steininger, M.K., Swenson, N.G., Uriarte, M., van Breugel, M., van der Wal, H., Veloso, M.D.M., Vester, H., Vieira, I.C.G., Bentos, T.V., Williamson, G.B., Poorter, L., 2016. Carbon sequestration potential of second-growth forest regeneration in the Latin American tropics. Sci. Adv. 2, e1501639.

Chen, G., Li, X., Liu, X., Chen, Y., Liang, X., Leng, J., Xu, X., Liao, W., Qiu, Y.a., Wu, Q., Huang, K., 2020. Global projections of future urban land expansion under shared socioeconomic pathways. Nat. Commun. 11, 537.

Chen, H., Zhu, Q., Peng, C., Wu, N., Wang, Y., Fang, X., Gao, Y., Zhu, D., Yang, G., Tian, J., Kang, X., Piao, S., Ouyang, H., Xiang, W., Luo, Z., Jiang, H., Song, X., Zhang, Y., Yu, G., Zhao, X., Gong, P., Yao, T., Wu, J., 2013. The impacts of climate change and human activities on biogeochemical cycles on the Qinghai-Tibetan Plateau. Glob. Chang. Biol. 19, 2940–2955.

Chen, J.M., Ju, W., Ciais, P., Viovy, N., Liu, R., Liu, Y., Lu, X., 2019. Vegetation structural change since 1981 significantly enhanced the terrestrial carbon sink. Nat. Commun. 10, 4259.

Chini, L., Hurtt, G., Sahajpal, R., Frolking, S., Goldewijk, K.K., Sitch, S., Ganzenmueller, R., Ma, L., Ott, L., Pongratz, J., Poulter, B., 2021. Land-use harmonization datasets for annual global carbon budgets. Earth Syst.Sci.Data 13, 4175–4189.

Ciais, P., Reichstein, M., Viovy, N., Granier, A., Ogee, J., Allard, V., Aubinet, M., Buchmann, N., Bernhofer, C., Carrara, A., Chevallier, F., De Noblet, N., Friend, A.D., Friedlingstein, P., Grunwald, T., Heinesch, B., Keronen, P., Knohl, A., Krinner, G., Loustau, D., Manca, G., Matteucci, G., Miglietta, F., Ourcival, J.M., Papale, D., Pilegaard, K., Rambal, S., Seufert, G., Soussana, J.F., Sanz, M.J., Schulze, E.D., Vesala, T., Valentini, R., 2005. Europe-wide reduction in primary productivity caused by the heat and drought in 2003. Nature 437, 529–533.

Cox, P.M., Pearson, D., Booth, B.B., Friedlingstein, P., Huntingford, C., Jones, C.D., Luke, C.M., 2013. Sensitivity of tropical carbon to climate change constrained by carbon dioxide variability. Nature 494, 341–344.

d'Amour, C.B., Reitsma, F., Baiocchi, G., Barthel, S., Guneralp, B., Erb, K.-H., Haberl, H., Creutzig, F., Seto, K.C., 2017. Future urban land expansion and implications for global croplands. Proc. Natl. Acad. Sci. U. S. A. 114, 8939–8944.

Di Vittorio, A.V., Mao, J., Shi, X., Chini, L., Hurtt, G., Collins, W.D., 2018. Quantifying the effects of historical land cover conversion uncertainty on global carbon and climate estimates. Geophys. Res. Lett. 45, 974–982.

Di Vittorio, A.V., Shi, X., Bond-Lamberty, B., Calvin, K., Jones, A., 2020. Initial land use/cover distribution substantially affects global carbon and local temperature projections in the integrated earth system model. Glob. Biogeochem. Cycles 34, e2019GB006383.

Donato, D.C., Kauffman, J.B., Murdiyarso, D., Kurnianto, S., Stidham, M., Kanninen, M., 2011. Mangroves among the most carbon-rich forests in the tropics. Nat. Geosci. 4, 293–297.

Dou, X., Lu, M., Chen, L., 2021. Comparison of soil organic carbon and nitrogen dynamics between urban impervious surfaces and vegetation. Land Degrad. Dev. 32, 5455–5467.

Doughty, C.E., Metcalfe, D.B., Girardin, C.A.J., Farfan Amezquita, F., Galiano Cabrera, D., Huaraca Huasco, W., Silva-Espejo, J.E., Araujo-Murakami, A., da Costa, M.C., Rocha, W., Feldpausch, T.R., Mendoza, A.L.M., da Costa, A.C.L., Meir, P., Phillips, O.L., Malhi, Y., 2015. Drought impact on forest carbon dynamics and fluxes in Amazonia. Nature 519, 78–U140.

Endreny, T.A., 2018. Strategically growing the urban forest will improve our world. Nat. Commun. 9, 1160.

Erb, K.-H., Fetzel, T., Plutzar, C., Kastner, T., Lauk, C., Mayer, A., Niedertscheider, M., Koerner, C., Haberl, H., 2016. Biomass turnover time in terrestrial ecosystems halved by land use. Nat. Geosci. 9, 674.

Erb, K.-H., Kastner, T., Plutzar, C., Bais, A.L.S., Carvalhais, N., Fetzel, T., Gingrich, S., Haberl, H., Lauk, C., Niedertscheider, M., Pongratz, J., Thurner, M., Luyssaert, S., 2018. Unexpectedly large impact of forest management and grazing on global vegetation biomass. Nature 553, 73.

Feng, Y., Wu, P., Tong, X., Li, P., Wang, R., Zhou, Y., Wang, J., 2022. The effects of factor generalization scales on the reproduction of dynamic urban growth. Geo-Spatial Inf. Sci. 25 (3), 457–475.

Gong, P., Li, X., Wang, J., Bai, Y., Cheng, B., Hu, T., Liu, X., Xu, B., Yang, J., Zhang, W., Zhou, Y., 2020. Annual maps of global artificial impervious area (GAIA) between 1985 and 2018. Remote Sens. Environ. 236, 111510.

Gregg, J.W., Jones, C.G., Dawson, T.E., 2003. Urbanization effects on tree growth in the vicinity of New York City. Nature 424, 183–187.

Guan, X., Shen, H., Li, X., Gan, W., Zhang, L., 2019. A long-term and comprehensive assessment of the urbanization-induced impacts on vegetation net primary productivity. Sci. Total Environ. 669, 342–352.

He, Q., Ju, W., Dai, S., He, W., Song, L., Wang, S., Li, X., Mao, G., 2021. Drought risk of global terrestrial gross primary productivity over the last 40 years detected by a remote sensing-driven process model. J.Geophys.Res.Biogeosci. 126, e2020JG005944.

Houghton, R.A., Nassikas, A.A., 2017. Global and regional fluxes of carbon from land use and land cover change 1850–2015. Glob. Biogeochem. Cycles 31, 456–472.

Huang, M., Piao, S., Ciais, P., Penuelas, J., Wang, X., Keenan, T.F., Peng, S., Berry, J.A., Wang, K., Mao, J., Alkama, R., Cescatti, A., Cuntz, M., De Deurwaerder, H., Gao, M., He, Y., Liu, Y., Luo, Y., Myneni, R.B., Niu, S., Shi, X., Yuan, W., Verbeeck, H., Wang, T., Wu, J., Janssens, I.A., 2019. Air temperature optima of vegetation productivity across global biomes. Nat.Ecol.Evol. 3, 772–779.

Huang, X., Li, J., Yang, J., Zhang, Z., Li, D., Liu, X., 2021. 30 m global impervious surface area dynamics and urban expansion pattern observed by Landsat satellites: from 1972 to 2019. Sci.ChinaEarth Sci. 64, 1922–1933.

Imhoff, M.L., Bounoua, L., DeFries, R., Lawrence, W.T., Stutzer, D., Tucker, C.J., Ricketts, T., 2004. The consequences of urban land transformation on net primary productivity in the United States. Remote Sens. Environ. 89, 434–443.

Jia, W., Zhao, S., Liu, S., 2018. Vegetation growth enhancement in urban environments of the conterminous United States. Glob. Chang. Biol. 24, 4084–4094.

Kern, R.A., Schlesinger, W.H., 1992. Carbon stores in vegetation. Nature 357, 447–448.

Lai, L., Huang, X., Yang, H., Chuai, X., Zhang, M., Zhong, T., Chen, Z., Chen, Y., Wang, X., Thompson, J.R., 2016. Carbon emissions from land-use change and management in China between 1990 and 2010. Sci. Adv. 2, e1601063.

Le Noe, J., Erb, K.-H., Matej, S., Magerl, A., Bhan, M., Gingrich, S., 2021. Altered growth conditions more than reforestation counteracted forest biomass carbon emissions 1990–2020. Nat. Commun. 12, 6075.

Li, W., Ciais, P., Peng, S., Yue, C., Wang, Y., Thurner, M., Saatchi, S.S., Arneth, A., Avitabile, V., Carvalhais, N., Harper, A.B., Kato, E., Koven, C., Liu, Y.Y., Nabel, J.E.M.S., Pan, Y., Pongratz, J., Poulter, B., Pugh, T.A.M., Santoro, M., Sitch, S., Stocker, B.D., Viovy, N., Wiltshire, A., Yousefpour, R., Zaehle, S., 2017a. Land-use and land-cover change carbon emissions between 1901 and 2012 constrained by biomass observations. Biogeosciences 14, 5053–5067.

Li, X., Gong, P., Zhou, Y., Wang, J., Bai, Y., Chen, B., Hu, T., Xiao, Y., Xu, B., Yang, J., Liu, X., Cai, W., Huang, H., Wu, T., Wang, X., Lin, P., Li, X., Chen, J., He, C., Li, X., Yu, L., Clinton, N., Zhu, Z., 2020. Mapping global urban boundaries from the global artificial impervious area (GAIA) data. Environ. Res. Lett. 15, 094044.

Li, Z., Jiao, L., Zhang, B., Xu, G., Liu, J., 2021. Understanding the pattern and mechanism of spatial concentration of urban land use, population and economic activities: a case study in Wuhan, China. Geo-Spat. Inf. Sci. 24, 678–694.

Li, X., Zhou, Y., Asrar, G.R., Mao, J., Li, X., Li, W., 2017b. Response of vegetation phenology to urbanization in the conterminous United States. Glob. Chang. Biol. 23, 2818–2830.

Liang, X., Liu, X., Li, X., Chen, Y., Tian, H., Yao, T., 2018. Delineating multi-scenario urban growth boundaries with a CA-based FLUS model and morphological method. Landsc. Urban Plan. 177, 47–63.

Liu, D., Li, H., Qiu, M., Liu, Y., 2022. Understanding coupled coordination relationships between social and ecological functions of urban green spaces. Geo-Spat. Inf. Sci. https://doi.org/10.1080/10095020.2022.2134057.

Liu, X., Pei, F., Wen, Y., Li, X., Wang, S., Wu, C., Cai, Y., Wu, J., Chen, J., Feng, K., Liu, J., Hubacek, K., Davis, S.J., Yuan, W., Yu, L., Liu, Z., 2019. Global urban expansion offsets climate-driven increases in terrestrial net primary productivity. Nat. Commun. 10, 5558.

Lu, M., Zou, Y., Xun, Q., Yu, Z., Jiang, M., Sheng, L., Lu, X., Wang, D., 2021. Anthropogenic disturbances caused declines in the wetland area and carbon pool in China during the last four decades. Glob. Chang. Biol. 27, 3837–3845.

Luo, Y., Sun, W., Yang, K., Zhao, L., 2021. China urbanization process induced vegetation degradation and improvement in recent 20 years. Cities 114, 103207.

Miettinen, J., Shi, C., Liew, S.C., 2011. Deforestation rates in insular Southeast Asia between 2000 and 2010. Glob. Chang. Biol. 17, 2261–2270.

Musikhin, I., Karpik, A., 2023. Use of GIS technology and cellular automata for modeling multiple socio-economic scenarios of regional spatial development and inter-regional cooperation. Geo-Spat. Inf. Sci. https://doi.org/10.1080/10095020.2023.2182237.

Qin, Y., Xiao, X., Wigneron, J.-P., Ciais, P., Brandt, M., Fan, L., Li, X., Crowell, S., Wu, X., Doughty, R., Zhang, Y., Liu, F., Sitch, S., Moore, B., 2021. Carbon loss from forest degradation exceeds that from deforestation in the Brazilian Amazon. Nat. Clim. Chang. 11, 442.

Quesada, B., Arneth, A., Robertson, E., de Noblet-Ducoudre, N., 2018. Potential strong contribution of future anthropogenic land-use and land-cover change to the terrestrial carbon cycle. Environ. Res. Lett. 13, 064023.

Seto, K.C., Guneralp, B., Hutyra, L.R., 2012. Global forecasts of urban expansion to 2030 and direct impacts on biodiversity and carbon pools. Proc. Natl. Acad. Sci. U. S. A. 109, 16083–16088.

Stocker, B.D., Zscheischler, J., Keenan, T.F., Prentice, I.C., Seneviratne, S.I., Penuelas, J., 2019. Drought impacts on terrestrial primary production underestimated by satellite monitoring. Nat. Geosci. 12, 264.

Surawski, N.C., Sullivan, A.L., Roxburgh, S.H., Meyer, C.P.M., Polglase, P.J., 2016. Incorrect interpretation of carbon mass balance biases global vegetation fire emission estimates. Nat. Commun. 7, 11536.

Tagesson, T., Schurgers, G., Horion, S., Ciais, P., Tian, F., Brandt, M., Ahlstrom, A., Wigneron, J.-P., Ardo, J., Olin, S., Fan, L., Wu, Z., Fensholt, R., 2020. Recent divergence in the contributions of tropical and boreal forests to the terrestrial carbon sink. Nat.Ecol.Evol. 4, 202–209.

Tang, L., Chen, X., Cai, X., Li, J., 2021. Disentangling the roles of land-use-related drivers on vegetation greenness across China. Environ. Res. Lett. 16, 124033.

Tian, C., Yue, X., Zhou, H., Lei, Y., Ma, Y., Cao, Y., 2021. Projections of changes in ecosystem productivity under 1.5 degrees C and 2 degrees C global warming. Glob. Planet. Chang. 205, 103588.

Tian, G., Qiao, Z., 2014. Assessing the impact of the urbanization process on net primary productivity in China in 1989–2000. Environ. Pollut. 184, 320–326.

Tong, Z., Yang, H., Liu, C., Xu, T., 2020. Quantification of the openness of urban external space through urban section. Geo-Spat. Inf. Sci. 23 (4), 316–326.

Wang, L., Tian, F., Wang, Y., Wu, Z., Schurgers, G., Fensholt, R., 2018. Acceleration of global vegetation Greenup from combined effects of climate change and human land management. Glob. Chang. Biol. 24, 5484–5499.

Wang, S., Ju, W., Penuelas, J., Cescatti, A., Zhou, Y., Fu, Y., Huete, A., Liu, M., Zhang, Y., 2019. Urban-rural gradients reveal joint control of elevated CO2 and temperature on extended photosynthetic seasons. Nat.Ecol.Evol. 3, 1076–1085.

Wen, Y., Liu, X., Bai, Y., Sun, Y., Yang, J., Lin, K., Pei, F., Yan, Y., 2019. Determining the impacts of climate change and urban expansion on terrestrial net primary production in China. J. Environ. Manag. 240, 75–83.

Wohlfahrt, G., Tomelleri, E., Hammerle, A., 2019. The urban imprint on plant phenology. Nat. Ecol.Evol. 3, 1668–1674.

Xu, C., McDowell, N.G., Fisher, R.A., Wei, L., Sevanto, S., Christoffersen, B.O., Weng, E., Middleton, R.S., 2019. Increasing impacts of extreme droughts on vegetation productivity under climate change. Nat. Clim. Chang. 9, 948.

Xu, X., Yang, G., Tan, Y., Tang, X., Jiang, H., Sun, X., Zhuang, Q., Li, H., 2017. Impacts of land use changes on net ecosystem production in the Taihu Lake Basin of China from 1985 to 2010. J.Geophys.Res.Biogeosci. 122, 690–707.

Yan, Y., Wu, C., Wen, Y., 2021. Determining the impacts of climate change and urban expansion on net primary productivity using the spatio-temporal fusion of remote sensing data. Ecol. Indic. 127, 107737.

Yao, Y., Wang, X., Li, Y., Wang, T., Shen, M., Du, M., He, H., Li, Y., Luo, W., Ma, M., Ma, Y., Tang, Y., Wang, H., Zhang, X., Zhang, Y., Zhao, L., Zhou, G., Piao, S., 2018. Spatiotemporal pattern of gross primary productivity and its covariation with climate in China over the last thirty years. Glob. Chang. Biol. 24, 184–196.

Yu, G., Wang, Q., Liu, Y., Liu, Y., 2011. Conceptual framework of carbon sequestration rate and potential increment of carbon sink of regional terrestrial ecosystem and scientific basis for quantitative carbon authentification. Prog. Geogr. 30, 771–787.

Zhang, L., Yang, L., Zohner, C.M., Crowther, T.W., Li, M., Shen, F., Guo, M., Qin, J., Yao, L., Zhou, C., 2022. Direct and indirect impacts of urbanization on vegetation growth across the world's cities. Sci. Adv. 8, eabo0095.

Zhao, S., Liu, S., Zhou, D., 2016. Prevalent vegetation growth enhancement in urban environment. Proc. Natl. Acad. Sci. U. S. A. 113, 6313–6318.

Zhuang, Q., Shao, Z., Li, D., Huang, X., Altan, O., Wu, S., Li, Y., 2022. Isolating the direct and indirect impacts of urbanization on vegetation carbon sequestration capacity in a large oasis city: evidence from Urumqi, China. Geo-Spat. Inf. Sci https://doi.org/10.1080/10095020.2022.2118624.

Qingwei Zhuang is a Ph.D candidate in the State Key Laboratory of Information Engineering in Surveying, Mapping and Remote Sensing, Wuhan University. He got master degrees from the University of Chinese Academy of Sciences. His research interest mainly focuses on remote sensing applications. The specific research directions include remote sensing image processing and analysis, key technologies and applications in urban ecosystem.

Zhenfeng Shao is a professor in State Key Laboratory of Information Engineering in Surveying, Mapping and Remote Sensing, Wuhan University. He got the PhD degree from Wuhan University in 2004. His research interest mainly focuses on urban remote sensing applications. The specific research directions include high-resolution remote sensing image processing and analysis, key technologies and applications from digital urban to smart urban and sponge urban.

Deren Li is a professor and chair of the Academic Committee of the State Key Laboratory for Information Engineering in Surveying, Mapping, and Remote Sensing, Wuhan University. He was selected as a member of Chinese Academy of Sciences in 1991 and a member of Chinese Academy of Engineering in 1994. He got his PhD degree from University of Stuttgart, Germany. He was awarded the title of honorary doctor from ETH, Switzerland in 2008. His research interests include photogrammetry and remote sensing, global navigation satellite system, geographic information system, and their innovation integrations and applications.

Xiao Huang is an Assistant Professor in the Department of Geoscience at the University of Arkansas. He obtained his Bachelor's degree from Wuhan University in 2015, Master's degree from Georgia Institute of Technology in 2016, and Ph.D. degree from University of South Carolina in 2020. His research interests cover big geospatial data, deep learning, applied remote sensing, and urban informatics.

Yuzhen Li is an associate professor in the School of Emergency Management at Xihua University. She received her PhD from the University of Chinese Academy of Sciences in 2020. Her research interests cover land surface models, terrestrial ecosystems and climate change, and remote sensing applications.

Orhan Altan is the Honorary Member of ISPRS and Science Academy, and Honorary Fellow of Indian Society of Remote Sensing. He received the master's degrees in civil engineering at Istanbul Polytechnic University in 1970. He studied at ETH Zurich Institute of Geodest and Photogrammetry from 1972 to 1973. He served as the director of ISPRS from 2000 to 2004. He was the secretary general of ISPRS from 2004 to 2008, chairman of ISPRS from 2008 to 2012; first vice chairman of ISPRS from 2012 to 2016; member of Executive Council of International Council of science from 2011 to 2018.

Shixin Wu is a professor in State Key Laboratory of Desert and Oasis Ecology, Xinjiang Institute of Ecology and Geography, Chinese Academy of Sciences. His research interests focus on land use and land cover change and its ecological environment effects.